

ORIGINAL ARTICLE

Towards a Best Practice Approach in PBPK Modeling: Case Example of Developing a Unified Efavirenz Model Accounting for Induction of CYPs 3A4 and 2B6

A Ke, Z Barter, K Rowland-Yeo and L Almond*

In this study, we present efavirenz physiologically based pharmacokinetic (PBPK) model development as an example of our best practice approach that uses a stepwise approach to verify the different components of the model. First, a PBPK model for efavirenz incorporating *in vitro* and clinical pharmacokinetic (PK) data was developed to predict exposure following multiple dosing (600 mg q.d.). Alfentanil i.v. and p.o. drug-drug interaction (DDI) studies were utilized to evaluate and refine the CYP3A4 induction component in the liver and gut. Next, independent DDI studies with substrates of CYP3A4 (maraviroc, atazanavir, and clarithromycin) and CYP2B6 (bupropion) verified the induction components of the model (area under the curve [AUC] ratios within 1.0–1.7-fold of observed). Finally, the model was refined to incorporate the fractional contribution of enzymes, including CYP2B6, propagating autoinduction into the model (Racc 1.7 vs. 1.7 observed). This validated mechanistic model can now be applied in clinical pharmacology studies to prospectively assess both the victim and perpetrator DDI potential of efavirenz.

CPT Pharmacometrics Syst. Pharmacol. (2016) 5, 367–376; doi:10.1002/psp4.12088; published online 20 July 2016.

Study Highlights

WHAT IS THE CURRENT KNOWLEDGE ON THE TOPIC?

Several efavirenz PBPK models have been used to support the clinical pharmacology reviews of new drug applications. There are literature reports that show the application of PBPK models to predict the interindividual variability in efavirenz PK and to support dose adjustment.

WHAT QUESTION DID THIS STUDY ADDRESS?

We sought to develop a unified mechanistic model for efavirenz that addresses both the victim (CYP2B6 induction) and perpetrator (CYP2B6 and CYP3A4 induction) properties of efavirenz.

WHAT THIS STUDY ADDS TO OUR KNOWLEDGE

We present our best practice approach for PBPK model development, using efavirenz as an example, where a stepwise “matrix” approach was used to verify the different components of the model.

HOW THIS MIGHT CHANGE DRUG DISCOVERY, DEVELOPMENT, AND/OR THERAPEUTICS

The mechanistic model for efavirenz can be applied in clinical pharmacology studies to prospectively assess its DDI potential. As the use of PBPK to simulate the impact of coadministration with moderate CYP3A4 inducers is commonplace, a unified and verified efavirenz PBPK model within the public domain can streamline PBPK packages in regulatory submissions.

Efavirenz is a non-nucleoside reverse transcriptase inhibitor. Daily therapy, including efavirenz (600 mg) with tenofovir (300 mg) and emtricitabine (200 mg) or lamivudine (300 mg), is recommended as an alternative treatment for human immunodeficiency virus-infected individuals aged ≥ 3 years, or first-line treatment in some populations, including pregnant women.¹ From a clinical pharmacology perspective, efavirenz is a well-known perpetrator of drug–drug interactions (DDIs) and one of the DDI properties of significant concern is moderate CYP3A4 induction. Efavirenz reduces the systemic exposures of coadministered, antiviral drugs, such as boceprevir, simeprevir, dolutegravir, amprenavir, and indinavir.^{2–6} As such, regulatory agencies expect the pharmaceutical industry to quantify the DDI potential of CYP3A4-substrate investigational drugs because of efavirenz coadministration, especially if the investigational drugs

are expected to be coprescribed in the target patient populations. One of the recently accepted approaches to quantify the DDIs perpetrated by efavirenz is the application of physiologically based pharmacokinetic (PBPK) modeling and simulation. In fact, several PBPK models for efavirenz were recently used to support the clinical pharmacology reviews of new drug applications with focus on assessing the modest CYP3A4 induction effect.^{7–9} There have been several studies in the literature that reported the application of PBPK models to predict the interindividual variability in efavirenz pharmacokinetics (PKs) due to CYP2B6 pharmacogenetics, and to support dose adjustment.^{10–12} A comparison of all available efavirenz models in the literature revealed that there are differences in several of the key model input parameters (e.g., plasma protein binding, CYP3A4/2B6 induction parameters). These differences

perhaps reflect the fact that many of these efavirenz models are “fit-for-purpose” and the aims of the simulations were different. Therefore, a unified mechanistic model that addresses both the victim and perpetrator properties of efavirenz is still lacking. Development of a mechanistic model for efavirenz requires accounting for all the key elements of absorption, distribution, metabolism, excretion and DDI properties, validating/verifying these key elements with independent datasets, and addressing any remaining uncertainty of key input parameters.

Efavirenz is a known victim of DDIs and a few drugs have been reported to induce (e.g., rifampin) or inhibit (e.g., voriconazole) efavirenz elimination.^{13,14} Efavirenz is predominantly cleared by hepatic metabolism and *in vitro* studies using human liver microsomes showed that CYP2B6 and CYP2A6 were the predominant CYPs involved in the formation of 8- and 7-hydroxyefavirenz, respectively.¹⁵ Clinical studies in patients with human immunodeficiency virus have repeatedly shown that CYP2B6 genetic variants with impaired function are associated with higher efavirenz exposure.^{16,17} Efavirenz induces its own clearance via the autoinduction of CYP2B6 upon multiple dosing.^{18,19} Thus, in order to construct a robust victim drug model, it is essential to obtain a robust estimate for the contribution (fm) of CYP2B6 and CYP3A4 to efavirenz clearance at baseline. In the absence of a clinical study with a strong CYP2B6 inhibitor, the fm_{CYP2B6} from *in vitro* metabolism data was verified by comparing the predicted autoinduction effect with observed data.

Efavirenz exhibits several DDI properties as a perpetrator. Efavirenz induces CYP2B6 activity *in vivo*, as demonstrated by a 2.3-fold increase in the area under the plasma concentration-time curve (AUC) ratio of hydroxybupropion: bupropion after 600 mg efavirenz administration for 2 weeks.²⁰ Efavirenz is a moderate inducer of CYP3A4 activity *in vivo*, as demonstrated by 1.9- and 4.5-fold increases in systemic and oral alfentanil clearances after efavirenz administration for 2 weeks (600 mg q.d.).¹⁸ In the literature, efavirenz induction of CYP3A4 activity has been quantitatively characterized in human hepatocytes and applied for *in vitro-in vivo* extrapolation (IVIVE) of CYP3A4 induction effect.²¹ Such data are sparse for CYP2B6 activity and successful IVIVE for CYP2B6 induction using a CYP2B6 marker substrate has not been shown.²² In the current study, we utilized CYP3A4 and CYP2B6 induction data measured in the same donors of human hepatocytes, to minimize interlaboratory and interdonor variability in the measured induction effect. In addition, organ-specific induction of hepatic but not intestinal CYP3A4 has been observed with efavirenz treatment, at least at the expression level,^{23,24} an apparent phenomenon that has remained unexplained.

Although the use of a workflow approach to develop PBPK models has been recommended,²⁵ a recent analysis of published PBPK models highlighted that important information is often missing.²⁶ The specific aim of this study was to demonstrate the use of a stepwise “matrix” approach in the development of a verified and unified PBPK model for efavirenz to: (1) predict the modest induction effect on CYP3A4 victim drugs; (2) predict the induction effect on CYP2B6 victim drugs; (3) predict single-dose and multiple-dose efavirenz PK considering the autoinduction effect.

METHODS

Simulations using PBPK modeling

The Simcyp (version 14.1) population-based PBPK simulator (Simcyp Ltd, Sheffield, UK) was used to simulate the PK of efavirenz and relevant DDIs with efavirenz in virtual healthy volunteers. The coefficient of variance (CV) for liver CYP2B6 abundance was modified from the Simcyp (version 14.1) default value of 122 to 60%, to better recover the PK variability for CYP2B6 substrates observed clinically (e.g., CV of 55% for efavirenz oral clearance at 600 mg q.d. dosing in 107 human immunodeficiency virus-infected patients genotyped as CYP2B6 extensive metabolizers).¹⁷

The metric for assessing predictive performance of PK parameters or DDIs was the predicted/observed ratio [= predicted mean exposure (ratio)/observed mean exposure (ratio)] fall within a predefined criterion of a 1.5-fold range. The exposure was defined as maximum plasma concentration (C_{max}) or AUC. Several success criteria (1.25-fold or 2-fold range) have been used in the literature.^{27–29} Here, a 1.5-fold range was chosen on the basis of the intrinsic PK variability of efavirenz,³⁰ as well as the moderate-to-mild extent of efavirenz perpetrated DDIs.²⁹

Development of efavirenz base model

Development of the base model is summarized below and described in full in **Supplementary Information**.

The 600 mg q.d. dosing regimen was the primary focus for model development because this is the recommended clinical dosing regimen. The model performance was also evaluated for 400 mg dose when data are available, as there is an effort to reduce efavirenz dosage to lower drug costs.¹⁷ The efavirenz model was developed based on *in vitro* data and refined using clinical PK data following oral administration. When data were obtained from more than one study, mean values were used.

The initial base model used *in vivo* oral clearance ($CL_{po} = 9.07$ L/h; 26% CV) (unpublished data provided by Bristol Myers Squibb) obtained from multiple dose administration as the clearance input. Volume of distribution at steady state (V_{ss}) was estimated from clinical data because of the uncertainty in efavirenz f_{up} and logP and the high sensitivity of the predicted V_{ss} to these parameters.³¹

In vitro CYP3A4 and CYP2B6 induction data, measured in the same donors ($n = 4$) of human hepatocytes, were incorporated into the model (**Supplementary Information**).

Base model verification

Simulations were run using the base model and CYP3A4 induction in the liver and gut was evaluated and refined based on the predicted effect of efavirenz 600 mg q.d. on alfentanil i.v. and p.o. PK. The simulated trial designs are described in **Supplementary Information**.

CYP3A4 induction in the refined model was then independently verified based on the prediction of the effect of efavirenz 600 mg q.d. on maraviroc, atazanavir, and clarithromycin PK. A published maraviroc model³² was used with one modification: predicted V_{ss} (= 1.7 L/kg) replaced observed V_{ss} and was used in the final model to better recover the observed maraviroc C_{max} following 100 mg

Table 1 Input parameter values used to simulate the kinetics of efavirenz

Parameter	Value	Method/comment
MW [g/mol]	315.68	http://www.drugbank.ca/drugs/DB00625
logP	4.02	Mean of measured values (range, 2.07–5.4) ^{12, 35–37}
pKa	10.2	Monoprotic acid ³⁸
f_u	0.029	Significant variability in measured values (range, 0.005–0.029), reported highest f_u value used ²¹
B:P ratio	0.74	Reported ³⁷
f_a	0.67	Reported ³³
k_a (hr^{-1})	0.14	Estimated from clinical data obtained following a single oral dose of 100 mg efavirenz (unpublished data provided by BMS)
T_{lag} (hr)	0.36	Estimated from clinical data obtained following a single oral dose of 100 mg efavirenz (unpublished data provided by BMS)
$F_{u,\text{gut}}$	0.005	Default value of 1 was used initially, optimized based on sensitivity analysis (see Results)
V_{ss} (L/kg) (minimal PBPK)	2.25	Estimated from clinical data due to the uncertainty in efavirenz f_{up} and logP
V_{sac} (L/kg)	1.1	Estimated from clinical data obtained following a single oral dose of 800 mg efavirenz (unpublished data provided by BMS)
k_{in} (hr^{-1})	0.29	Estimated from clinical data obtained following a single oral dose of 800 mg efavirenz (unpublished data provided by BMS)
k_{out} (hr^{-1})	0.36	Estimated from clinical data obtained following a single oral dose of 800 mg efavirenz (unpublished data provided by BMS)
CL_{R} (L/h)	0	Reported
Single-dose CL/F (L/h)	5.87	Mean value observed after the administration of a single oral dose to 600 mg to healthy volunteers ^{15,19}
Enzyme kinetics – CYP2B6 CL_{int} ($\mu\text{l}/\text{min}/\text{pmol}$)	1.36	Retrograde calculation – assign 62% of hepatic CL
CYP2A6 CL_{int} ($\mu\text{l}/\text{min}/\text{pmol}$)	0.46	Retrograde calculation – assign 26.6% of hepatic CL
CYP1A2 CL_{int} ($\mu\text{l}/\text{min}/\text{pmol}$)	0.03	Retrograde calculation – assign 4.6% of hepatic CL
CYP3A4 CL_{int} ($\mu\text{l}/\text{min}/\text{pmol}$)	0.012	Retrograde calculation – assign 4.6% of hepatic CL
Additional HLM CL_{int} ($\mu\text{l}/\text{min}/\text{mg}$)	0.694	Retrograde calculation – assign 2% of hepatic CL
CYP2B6 IndC_{50} (μM)	1.2	Determined in human hepatocytes based on activity levels and not calibrated ³⁹ ; $f_{u,\text{inc}}$ of 0.15 was applied (see below)
CYP2B6 Ind_{max} (fold)	6.2	Determined in human hepatocytes based on activity levels ³⁹ and not calibrated
CYP3A4 IndC_{50} (μM)	3.8	Determined in human hepatocytes based on mRNA levels and calibrated against rifampin data ³⁴ ; $f_{u,\text{inc}}$ of 0.15 was applied based on sensitivity analysis in the range of 0.1–0.5 (per experiment values)
CYP3A4 Ind_{max} (fold)	9.9	Determined in human hepatocytes based on mRNA levels and calibrated against rifampin data ³⁴

MW, molecular weight; logP, log octanol/buffer partition coefficient (neutral species); B:P, blood-to-plasma ratio; f_a , fraction absorbed; k_a , absorption rate constant; BMS, Bristol Myers Squibb; V_{ss} , volume of distribution at steady state; PBPK, physiologically based V_{sac} , volume of the single-adjusting compartment; k_{in} and k_{out} , first order rate constants which act on the masses of drug within the systemic compartment and the SAC respectively; CL_{R} , renal clearance; CL/F, oral clearance; CL_{int} , intrinsic clearance; IndC_{50} , inducer concentration that support half maximal induction; HLM, human liver microsome; $F_{u,\text{inc}}$, the fraction unbound in an *in vitro* hepatocyte incubation.

b.i.d. dosing in healthy volunteers (simulated trial design in **Supplementary Information**).

CYP2B6 induction was then verified based on prediction of the effect of efavirenz 600 mg q.d. on bupropion p.o. PK (simulated trial design in **Supplementary Information**).

Development of efavirenz final model

The final input parameters for the model are summarized in **Table 1**.^{12,15,19,21,33–39} Final model development is summarized below and full details are provided in **Supplementary Information**.

The absorption following a daily oral dose of efavirenz was described as a first-order process after a lag time ($t_{\text{lag}} = 0.36$ h) with fraction absorbed of 0.67³³ and absorption rate constant of 0.41 h^{-1} . The absorption rate

constant and t_{lag} were estimated from fitting the clinical kinetic data obtained following a single oral dose of 100 mg efavirenz (unpublished data provided by Bristol Myers Squibb).

A minimal PBPK model⁴⁰ with a single-adjustment compartment (SAC) was used as the distribution model. The addition of an single-adjustment compartment was necessary to recover the shape of the plasma concentration-time profiles beyond 24 hours postdosing. The estimated V_{sac} is 1.1 L/kg associated with k_{in} and k_{out} of 0.29 and 0.09 hour^{-1} , respectively.

In vitro data describing the enzyme kinetics for efavirenz in human liver microsomes,^{15,41} underpredicted clearance and so were not used in the final model. Instead, input parameters for CL_{int} were back-calculated from observed mean CL_{po} (= 5.87 L/hr; single dose)^{15,19} using fm data

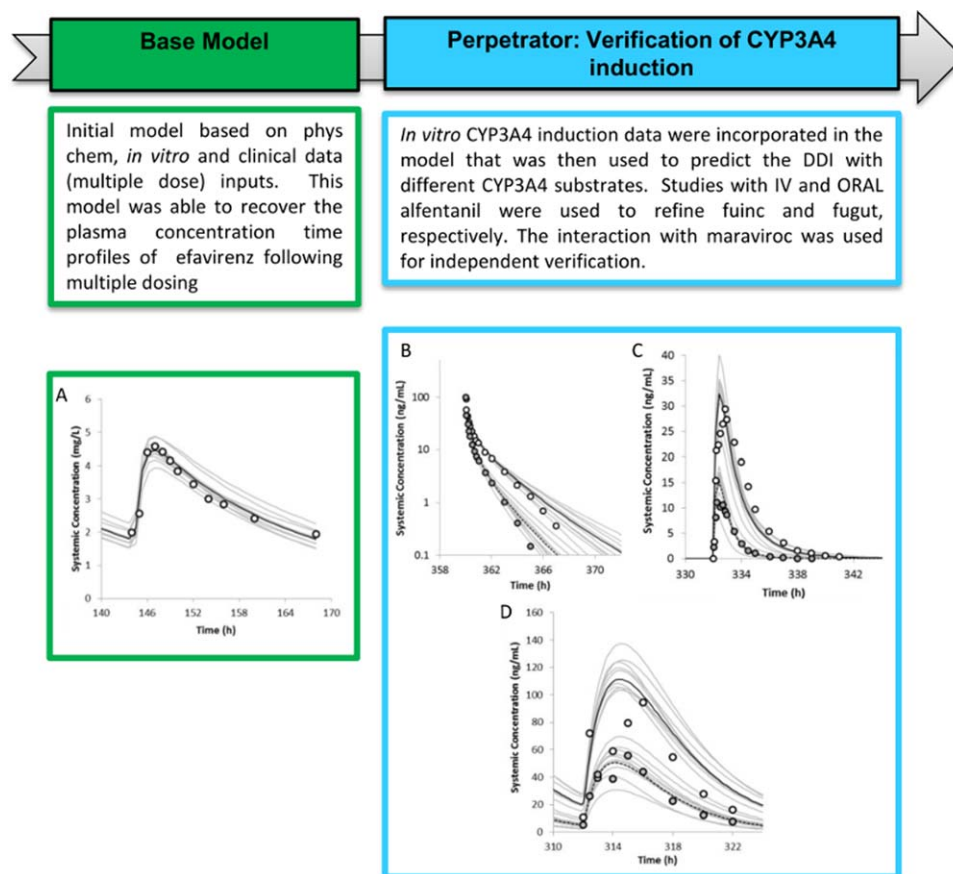


Figure 1 The workflow of efavirenz model development with a focus on the CYP3A4 induction component. (a) Simulated mean (solid black line) and observed (data points, Bristol Myers Squibb) mean plasma concentrations of efavirenz on day 7 following daily oral dosing of 600 mg efavirenz to healthy volunteers. The observed *in vivo* CL_{PO} was used as clearance input. (b) Simulated mean and observed (data points, Kharasch *et al.*,¹⁸ 2012) mean plasma concentrations of alfentanil on day 16 following 15 $\mu\text{g}/\text{kg}$ i.v. bolus in the absence (solid black line) and presence (dashed line) of efavirenz treatment (600 mg q.d. for 20 days) in healthy volunteers. The predicted alfentanil (i.v.) area under the curve (AUC) ratio of 0.56 (90% confidence interval [CI] = 0.55–0.58) was comparable to the observed AUC ratio of 0.54 (90% CI = 0.47–0.62). (c) Simulated mean and observed (data points, Kharasch *et al.*,¹⁸ 2012) mean plasma concentrations of alfentanil on day 15 following a single oral dose of 43 $\mu\text{g}/\text{kg}$ in the absence (solid black line) and presence (dashed line) of efavirenz treatment (600 mg q.d. for 20 days) in healthy volunteers. The predicted alfentanil (p.o.) AUC ratio of 0.28 (90% CI = 0.26–0.30) was comparable to the observed AUC ratio of 0.22 (90% CI = 0.16–0.30). (d) Simulated mean and observed (Abel *et al.*,³⁷ 2008) mean plasma concentrations of maraviroc on day 14 following 100 mg b.i.d. for 14 days in the absence (solid black line) and presence (dashed line) of efavirenz treatment (600 mg q.d. for 14 days) in healthy volunteers. The predicted maraviroc AUC ratio and C_{max} ratio were 0.38 (90% CI = 0.36–0.40) and 0.44 (90% CI = 0.42–0.46), respectively, compared to the observed AUC ratio of 0.49 (90% CI = 0.41–0.57) and C_{max} ratio of 0.44 (90% CI = 0.30–0.62). The gray lines represent the individual trials.

derived from *in vitro* data.¹⁵ The contribution of CYP2B6, 2A6, 1A2, and 3A4 to efavirenz metabolism was assigned to 62%, 26.6%, 4.6%, and 4.6%, respectively. Although there are no suitable clinical DDI studies with a strong inhibitor of CYP2B6 to independently verify the fm_{CYP2B6} , the minor contribution of CYP3A4 is consistent with an itraconazole DDI study demonstrating negligible effect on efavirenz PK, albeit in Korean subjects.⁴²

Final model verification

The final model was verified based on the prediction of the kinetics of efavirenz following single or multiple oral doses. Plasma concentration-time profiles and PK parameters (400 mg and 600 mg q.d. data) provided by Bristol Myers Squibb were used.

RESULTS

Workflow for model development and verification strategy

The model development and verification strategy are outlined in **Figures 1 and 2**. The initial step involved assessment and optimization of CYP3A4-mediated induction by efavirenz as the perpetrator using clinical kinetic data to drive the model. Alfentanil (both i.v. and oral formulations) was used as the CYP3A4 victim drug. The resultant model was then applied to predict DDIs involving other CYP3A4 drugs, including maraviroc, atazanavir, and clarithromycin to verify the CYP3A4 induction component. A bupropion DDI study was evaluated to verify the *in vitro* CYP2B6 induction component of the file. Finally, the efavirenz base model was subsequently expanded by incorporating fm_{CYP2B6} (62%) derived from *in*

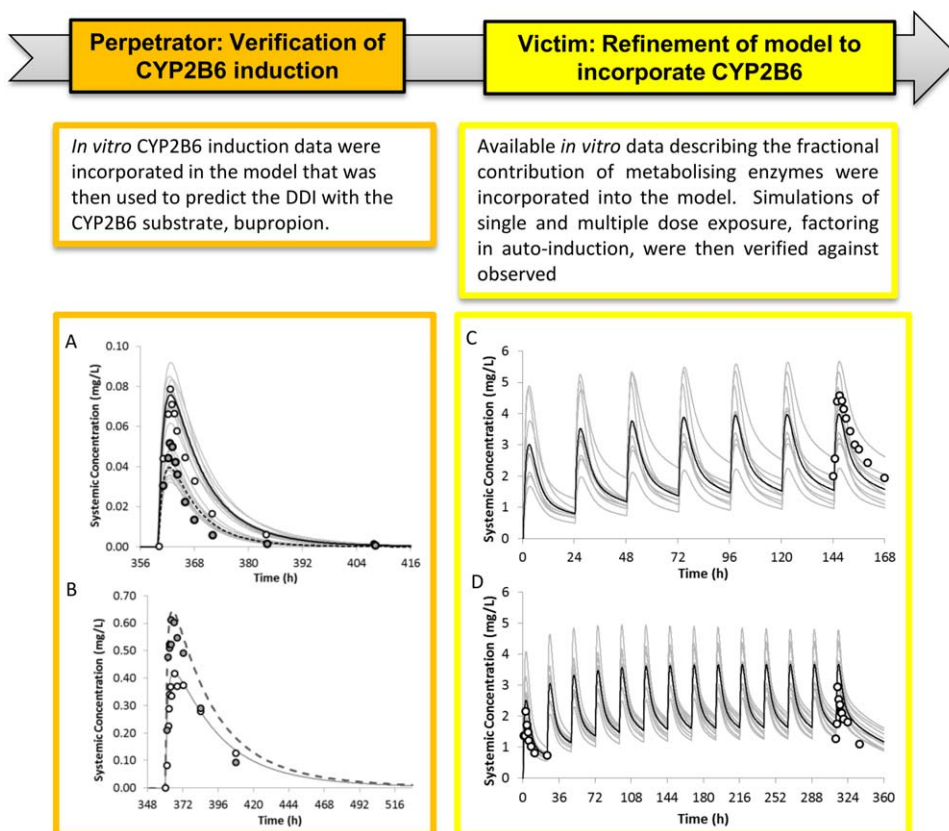


Figure 2 The workflow of efavirenz model development with a focus on the CYP2B6 induction component and fm_{CYP2B6} . Simulated mean and observed (Robertson *et al.*,²⁰ 2008) mean plasma concentrations of bupropion (**a**) and hydroxybupropion (**b**) on day 16 following a single oral dose of 150 mg bupropion in the absence (solid black line) and presence (dashed line) of efavirenz treatment (600 mg q.d. for 15 days) in healthy volunteers. The predicted bupropion (p.o.) AUC ratio and C_{max} ratio were 0.45 (90% CI = 0.42–0.46) and 0.50 (90% CI = 0.49–0.53), comparable to the observed AUC ratio of 0.45 (90% CI = 0.38–0.52) and C_{max} ratio of 0.66 (90% CI = 0.53–0.79). The predicted hydroxybupropion (p.o.) AUC ratio and C_{max} ratio were 1.44 (90% CI = 1.42–1.53) and 1.58 (90% CI = 1.57–1.68), compared with the observed AUC ratio of 1.0 (90% CI = 0.81–1.2) and C_{max} ratio of 1.5 (90% CI = 1.2–1.8). (**c**) Simulated mean (solid black line) and observed (data points: Bristol Myers Squibb) mean plasma concentrations of efavirenz on day 7 following daily oral dosing of 600 mg efavirenz to healthy volunteers. The predicted day 7 efavirenz AUC_{0–24} and C_{max} were 57.7 (CV%: 74) mg/L.h and 4.1 (CV%: 65) mg/L, compared with the observed AUC_{0–24} of 70.6 (CV%: 27) mg/L.h and C_{max} of 4.8 (CV%: 21) mg/L.h. (**d**) Simulated mean (solid black line) and observed (data points: Kharasch *et al.*,¹⁸ 2012) mean plasma concentrations of efavirenz on day 1 and 14 following daily oral dosing of 600 mg efavirenz to healthy volunteers. The predicted day 14 efavirenz AUC_{0–24} and C_{max} were 59 (CV%: 87) mg/L.h and 3.7 (CV%: 55) mg/L, compared with the observed AUC_{0–24} of 42.2 mg/L.h and C_{max} of 3.0 mg/L.h. The gray lines represent the individual trials.

in vitro metabolism data and CYP2B6 induction data. The predictive performance for single-dose and multiple-dose efavirenz pharmacokinetics, considering the autoinduction effect, was then verified. Each step of the model development/verification is explained in detail below.

Evaluation and refinement of CYP3A4 induction in the liver and gut: prediction of the effect of efavirenz 600 mg q.d. on alfentanil i.v. and p.o. kinetics

The developed efavirenz base model was able to recover the steady-state systemic exposure of efavirenz after a 600 mg once daily dosing to healthy volunteers (**Figure 1a**). To evaluate efavirenz induction effect on hepatic and intestinal CYP3A4 activity, the effect of efavirenz (600 mg q.d. for 20 days) on a CYP3A4 marker substrate, alfentanil (15 μ g/kg i.v. bolus on

day 16, and 43 μ g/kg p.o. on day 15) was simulated based on the studies of Kharasch *et al.*¹⁸ in 2012.

Efavirenz caused organ-specific induction of hepatic but not intestinal CYP3A4, at least at the expression level.^{14,15} Because efavirenz is highly bound to plasma proteins and is fairly lipophilic, we hypothesized that this phenomenon may be related to the unbound drug concentration that is available for interaction at the respective enzyme site. We tested this hypothesis by optimizing the relevant fraction unbound values in the incubation ($f_{u,inc}$) and gut ($f_{u,gut}$) and comparing the predicted alfentanil i.v. and p.o. AUC ratio due to efavirenz treatment with reported data. A sensitivity analysis of $f_{u,inc}$ in the range of 0.1–0.5 was conducted to evaluate its effect on the predicted alfentanil i.v. AUC ratio (**Figure 3a**). The results

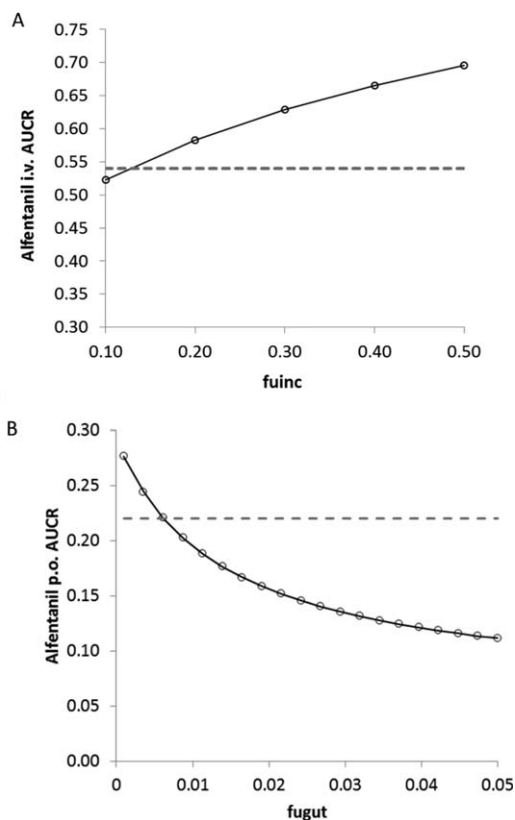


Figure 3 (a) Sensitivity analysis of $f_{u,inc}$ in the range of 0.1–0.5 to evaluate its effect on the predicted alfentanil i.v. area under the curve (AUC) ratio. (b) Sensitivity analysis of $f_{u,gut}$ in the range of 0.001–0.05 to evaluate its effect on the predicted alfentanil p.o. AUC ratio. The dashed lines represent the observed mean AUC ratios.

indicated that an $f_{u,inc}$ of 0.15 best recovered the observed alfentanil i.v. AUC ratio; the predicted AUC ratio of 0.56 (90% confidence interval [CI] = 0.55–0.58) was comparable to the observed AUC ratio of 0.54 (90% CI = 0.47–0.62; **Figure 1b**). This value was also in line with measured $f_{u,inc}$ values (range, 0.1–0.2) from two independent laboratories (personal communications with Ruben de Kanter, Actelion, Switzerland and Odette Fahmi and Keith Riccardi, Pfizer, Groton, CT).

Application of the efavirenz base model ($f_{u,gut} = 1$) resulted in a significant overprediction of the alfentanil p.o. AUC ratio: the predicted AUC ratio was 0.08 vs. an observed AUC ratio of 0.22. This result suggests that when not accounting for binding in the intestine, the induction of intestinal CYP3A4 was overpredicted. Sensitivity analysis (**Figure 3b**) showed that when $f_{u,gut}$ was set to the lowest reported f_{up} (= 0.005), the predicted alfentanil (p.o.) AUC ratio was 0.28 (90% CI = 0.26–0.30), which was comparable to the observed AUC ratio of 0.22 (90% CI = 0.16–0.30; **Figure 1c**). The corresponding changes in active CYP3A4 are 3.3-fold and 1.5-fold induction in the liver and gut, respectively (**Figure 4a,b**). The differential CYP3A4 induction profiles in the liver and gut are conceptually consistent with the findings that efavirenz (400 mg q.d.) caused organ-specific induction of hepatic but not intestinal CYP3A4 at the expression level.^{23,24}

Independent verification of CYP3A4 induction: prediction of the effect of efavirenz 600 mg q.d. on maraviroc, atazanavir, and clarithromycin PKs

The alfentanil, maraviroc, atazanavir, and clarithromycin models were independently verified with ketoconazole DDI studies (**Supplementary Information**).

The effect of efavirenz treatment (600 mg q.d. for 14 days) on maraviroc systemic exposures (100 mg b.i.d. for 14 days) were simulated (**Figure 1d**). The predicted maraviroc AUC ratio and C_{max} ratio were 0.38 (90% CI = 0.36–0.40) and 0.44 (90% CI = 0.42–0.46), respectively, compared to the observed AUC ratio of 0.49 (90% CI = 0.41–0.57) and C_{max} ratio of 0.44 (90% CI = 0.30–0.62).⁴³ The model predictions were within 1.3-fold of the observed values (**Table 2**).

The effect of efavirenz treatment (600 mg q.d. on days 7–20) on atazanavir systemic exposures (400 mg q.d. for 20 days) was simulated. The predicted atazanavir AUC ratio and C_{max} ratio were 0.43 (90% CI = 0.40–0.47) and 0.57 (90% CI = 0.54–0.61), respectively, compared to the observed AUC ratio of 0.26 (90% CI = 0.22–0.32) and C_{max} ratio of 0.41 (90% CI = 0.33–0.51).⁴⁴ The model predictions were within 1.7-fold of the observed values (**Table 2**).

The effect of efavirenz treatment (400 mg q.d. for 7 days) on clarithromycin systemic exposures (500 mg every 12 hours for 7 days) was simulated. The predicted clarithromycin AUC ratio and C_{max} ratio were 0.36 (90% CI = 0.32–0.39) and 0.54 (90% CI = 0.51–0.57), respectively, compared to the observed AUC ratio of 0.61 (90% CI = 0.54–0.70) and C_{max} ratio of 0.74 (90% CI = 0.65–0.85).⁴⁴ The model predictions were within 1.7-fold of the observed values (**Table 2**).

Verification of CYP2B6 induction: prediction of the effect of efavirenz 600 mg q.d. on bupropion p.o. kinetics

To independently verify the efavirenz induction effect on CYP2B6, the effect of efavirenz (600 mg q.d. for 15 days) on bupropion (150 mg p.o. on day 16) was simulated based on the study of Robertson *et al.*²⁰ in 2008. The predicted bupropion (p.o.) AUC ratio and C_{max} ratio were 0.44 (90% CI = 0.42–0.46) and 0.51 (90% CI = 0.49–0.53), comparable to the observed AUC ratio of 0.45 (90% CI = 0.38–0.52) and C_{max} ratio of 0.66 (90% CI = 0.53–0.79; **Figure 2a and Table 2**). The predicted hydroxybupropion (p.o.) AUC ratio and C_{max} ratio were 1.44 (90% CI = 1.42–1.53) and 1.58 (90% CI = 1.57–1.68), vs. the observed AUC ratio of 1.0 (90% CI = 0.81–1.2) and C_{max} ratio of 1.5 (90% CI = 1.2–1.8; **Figure 2b and Table 2**).

When competitive inhibition of CYP2B6 (K_i : 2.96 μ M) and CYP3A4 (K_i : 40.3 μ M)⁴⁵ was included into the model, there was little or no impact on predicted interaction ratios (e.g., predicted bupropion AUC ratio and C_{max} ratio 0.45 (90% CI = 0.43–0.47) and 0.52 (90% CI = 0.49–0.53); maraviroc AUC ratio and C_{max} ratio 0.39 (90% CI = 0.37–0.40) and 0.44 (90% CI = 0.42–0.46); alfentanil (p.o.) AUC ratio and C_{max} ratio 0.28 (90% CI = 0.26–0.30) and 0.43 (90% CI = 0.41–0.46). As a lack of DDI studies using single dose

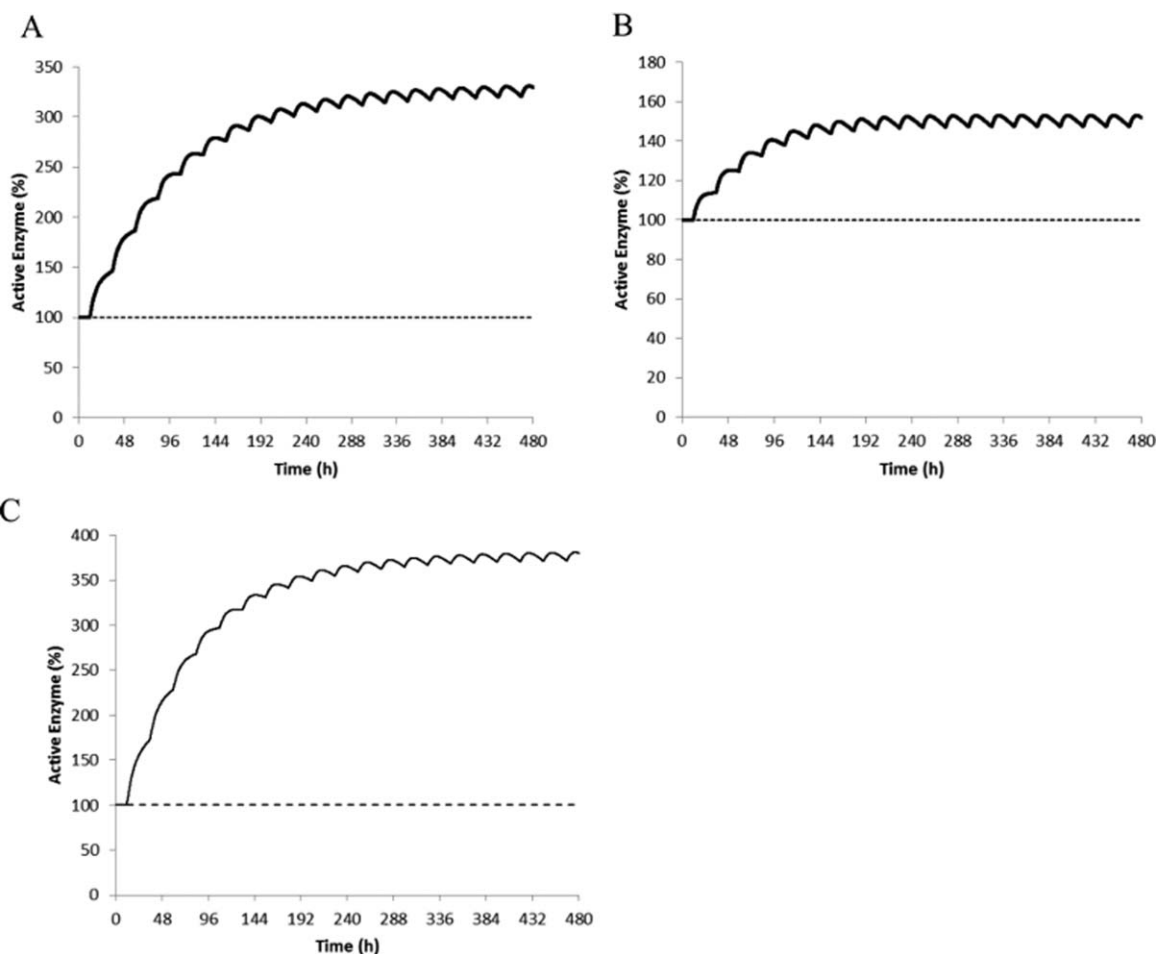


Figure 4 Predicted mean levels of active CYP3A4 in the liver (a), gut (b), and CYP2B6 in the liver (c) during 20 days of dosing with efavirenz (600 mg daily).

Table 2 Summary of DDI simulations of efavirenz treatment on victim drugs

Victim drugs dosing regimen ^a	AUC ratio			C _{max} ratio		
	Observed GMR (90% CI)	Predicted GMR (90% CI)	Predicted/observed	Observed GMR (90% CI)	Predicted GMR (90% CI)	Predicted/observed
Bupropion 150 mg p.o.	0.45 (0.38–0.52)	0.44 (0.42–0.46)	0.98	0.66 (0.53–0.79)	0.51 (0.49–0.53)	0.77
Bupropion 150 mg p.o. ^b	0.45 (0.38–0.52)	0.45 (0.43–0.47)	1.00	0.66 (0.53–0.79)	0.52 (0.50–0.54)	0.79
Alfentanil 43 µg/Kg p.o.	0.22 (0.16–0.30)	0.28 (0.26–0.30)	1.27	0.43 –	0.44 (0.41–0.46)	1.03
Maraviroc 100 mg b.i.d.	0.49 (0.41–0.57)	0.38 (0.36–0.40)	0.78	0.44 (0.30–0.62)	0.44 (0.42–0.46)	1.00
Atazanavir 400 mg q.d.	0.26 (0.22–0.32)	0.43 (0.40–0.47)	1.65	0.41 (0.33–0.51)	0.57 (0.54–0.61)	1.39
Clarithromycin 500 mg b.i.d.	0.61 (0.54–0.70)	0.36 (0.32–0.39)	0.59	0.74 (0.65–0.85)	0.54 (0.51–0.57)	0.73

AUC, area under the curve; CI, confidence interval; C_{max}, peak plasma concentration; DDI, drug-drug interaction; GMR, geometric mean ratio.
^aThe efavirenz dosing regimen used was 600 mg q.d. for at least 14 days, except for the clarithromycin DDI, in which the efavirenz dosing regimen was 400 mg q.d. for 7 days. ^bThis simulation incorporated the *in vitro* CYP2B6 Ki of 2.96 µM for efavirenz determined in pooled human liver microsomes.⁴⁵

Table 3 Mean predicted and observed C_{\max} and AUC values of efavirenz following various dosing regimens

Efavirenz dose	AUC _{0-inf} or AUC ₀₋₂₄ (mg/L.h)			C_{\max} (mg/L)		
	Observed mean (CV%)	Predicted mean (CV%)	Predicted/observed	Observed mean (CV%)	Predicted mean (CV%)	Predicted/observed
400 mg single dose	79.2 ^a (44)	57.6 (59)	0.73	1.4 ^a (12)	2.1 (96)	1.50
400 mg q.d. for 10 days	50.7 ^b (39)	46.9 (69)	0.92	3.4 ^b (29)	3.1 (70)	0.91
600 mg single dose	80.6 ^c –	80.6 (60)	1.00	2.5 ^c –	3.0 (95)	1.20
600 mg q.d. for 7 days	70.6 ^a (27)	57.7 (74)	0.82	4.8 ^a (21)	4.1 (65)	0.86
600 mg q.d. for 14 days	42.4 ^d –	59 (87)	1.39	3.0 ^d –	3.7 (55)	1.25

AUC, area under the curve; C_{\max} , peak plasma concentration; CV%, coefficient of variance percentage.

^aObserved data provided by BMS. ^bObserved data from Liu *et al.*,¹³ 2008. ^cMean C_{\max} and AUC values were not provided in Ogburn *et al.*,¹⁵ 2010. The values shown were estimated from the reported mean concentration-time profile. ^dMean C_{\max} and AUC values were not provided in Kharasch *et al.*,¹⁸ 2012. The values shown were estimated from the reported mean concentration-time profile.

efavirenz means the effect of competitive inhibition *in vivo* cannot be verified and knowing the overall impact on the predicted DDI is negligible, competitive inhibition was not included in the final model.

Verification of final model: prediction of the kinetics of efavirenz following single or multiple oral doses

The efavirenz base model was expanded to include fm data derived from human liver microsome data (see **Supplementary Information**). Mean simulated and observed plasma efavirenz concentrations following daily dosing of 600 mg efavirenz for 7–14 days are overlaid in **Figure 2c** (day 7) and **Figure 2d** (day 1 and 14). Simulated and observed mean C_{\max} and AUC values of efavirenz following 400 to 600 mg single dose and multiple dose of efavirenz are shown in **Table 3**. The predicted/observed mean C_{\max} ranged from 0.86–1.50, and the mean AUC ranged from 0.73–1.39. The model based on *in vitro* induction parameters determined in human hepatocytes, predicted 1.7-fold autoinduction of efavirenz oral clearance following efavirenz 600 mg q.d. for 7–14 days, consistent with the reported 1.6- to 1.7-fold autoinduction in efavirenz oral clearance following 600 mg q.d. for 14 days.^{18,19}

DISCUSSION

In the current study, we sought to develop a unified mechanistic model for efavirenz that addresses both the victim (CYP2B6 induction) and perpetrator (CYP2B6 and CYP3A4 induction) properties of efavirenz that, in turn, accounts for its changing clearance on multiple dosing due to autoinduction. Although this is not the first report of a PBPK model for efavirenz, we believe it is the first model that (1) demonstrates adequate predictive performance for CYP3A4 and CYP2B6 induction as well as autoinduction, and (2) accounts for organ-specific induction of CYP3A4 by verifying the model predictions with independent clinical datasets. Furthermore, in response to calls for standardization of PBPK model development and verification,^{26,46} we provide this as a case study demonstrating our recommended

workflow for the development of complex models for the application of DDI prediction.

During model development, three drug-specific parameters were identified to be associated with significant variability or uncertainty: $f_{u,p}$, $f_{u,inc}$, and $f_{u,gut}$. The $f_{u,p}$ is a key parameter that feeds into the prediction of CL_{po} , V_{ss} , and DDIs. To address the variability in reported $f_{u,p}$, we constructed a base model for efavirenz using *in vivo* CL_{po} and V_{ss} to recover the steady-state systemic exposures of efavirenz following multiple daily doses of 600 mg. This “model reduction” approach was necessary to allow the evaluation of CYP3A4 induction in isolation from all other confounding factors. The highest reported $f_{u,p}$ value was required in the final model to predict any appreciable CYP3A4 induction *in vivo*. The $f_{u,inc}$ is the free fraction in the *in vitro* incubation that impacts on the unbound $IndC_{50}$. The $f_{u,gut}$ is the free fraction of drug in the enterocyte that is available for metabolism, inhibition, and induction. The optimization of $f_{u,inc}$ and $f_{u,gut}$ values, based on both alfentanil i.v. and p.o. DDI data, respectively, ensured that the developed model captured the differential CYP3A4 induction profiles in the liver and intestine. The uncertainty around $f_{u,inc}$ was further resolved experimentally by obtaining two independent measurements, one using the same protocol as used in the hepatocyte induction experiments.³⁴ The uncertainty around $f_{u,gut}$, on the other hand, cannot be resolved experimentally. This is because nonspecific binding values generated in intestinal tissue homogenates do not account for physiological factors, such as the villous blood flow maintaining a “sink” condition. Uncertainty in $f_{u,gut}$ was therefore, addressed through sensitivity analysis and verification with alfentanil p.o. DDI data. Once these identified issues had been addressed, the efavirenz base model was subsequently expanded by incorporating CYP2B6 induction data, and verified with a bupropion DDI study, before finally the fm_{CYP2B6} derived from *in vitro* data were included.

A “matrix approach” was used to independently verify the perpetrator properties of efavirenz: (1) alfentanil i.v. and p.o. DDI studies were utilized to refine CYP3A4 induction component; (2) maraviroc, atazanavir, and clarithromycin

DDI studies were utilized to verify CYP4A4 induction component; and (3) bupropion DDI study was evaluated to verify the CYP2B6 induction component. All victim drug models were independently verified with clinical DDI data (**Supplementary Information**) before these models were used to evaluate the efavirenz DDI predictions. Application of the efavirenz model to predict the DDI magnitude following dosing of multiple CYP3A4 substrate drugs showed acceptable prediction of mavarivoc (1.3-fold), atazanavir (1.7-fold), and clarithromycin DDI (1.7-fold). Although prediction accuracy in terms of mean predicted vs. observed AUC ratios varied across CYP3A substrates, no systematic under or overprediction of CYP3A4-mediated DDIs was observed. It is important to note that both atazanavir and clarithromycin are potent CYP3A4 mechanism-based inhibitors. Therefore, the DDI mechanisms are more complex than those involved in the alfentanil and maraviroc DDI. For this reason, the model predictions being within twofold of the observed DDIs were deemed to be acceptable.^{27,46} The efavirenz model successfully predicted the bupropion DDI magnitude with coadministration of multiple oral dosing of 600 mg efavirenz. To our knowledge, successful IVIVE of CYP2B6 induction by efavirenz using a CYP2B6 marker substrate, such as bupropion, has not been shown in the literature. Interestingly, the predicted 1.4-fold increase in hydroxybupropion (p.o.) AUC vs. the observed negligible effect on hydroxybupropion AUC, indicates that the elimination of hydroxybupropion (by unknown mechanisms) may be induced by efavirenz treatment, which was not considered in the simulation. Overall, in 8 of 10 (AUC or AUC ratio) and 9 of 9 (C_{\max} or C_{\max} ratio) of the cases, the predictions were within the predefined 1.5-fold range. In 4 of 10 (AUC or AUC ratio) and 4 of 9 (C_{\max} or C_{\max} ratio) of the cases, the predictions were within a more stringent criterion of a 1.25-fold range.

The developed efavirenz model, incorporating $f_{mCYP2B6}$ (62%) derived from *in vitro* metabolism data, and CYP2B6 and CYP3A4 induction data obtained from the same human hepatocytes donors, predicted 1.7-fold autoinduction of efavirenz oral clearance following efavirenz 600 mg q.d. for 7–14 days. This is consistent with the reported 1.6- to 1.7-fold autoinduction of efavirenz oral clearance following 14 days of 600 mg q.d.^{18,19} One limitation of the efavirenz model is that $f_{mCYP2B6}$ derived from *in vitro* data is considered to be associated with uncertainty, due to the cross-reactivity of ticlopidine with CYP2C19.⁴⁷ Here, the successful prediction of the extent of autoinduction provided verification of $f_{mCYP2B6}$ for efavirenz, albeit to a limited extent. Literature models^{7,8,22} based on CYP2B6 and CYP3A4 induction parameters obtained from different human hepatocytes donors, predicted autoinduction effect of nearly threefold, which may indicate an overprediction of the CYP2B6 induction effect or error in $f_{mCYP2B6}$. Alternatively, the discrepancy in the estimated magnitude of autoinduction from clinical data may stem from the variability in single-dose PK parameters, and selections of clinical studies that reported both single-dose and multiple-dose PK in the same individuals.

Unlike IVIVE of CYP3A4 induction, for which an *in vivo* calibrator (i.e., rifampin) has been developed and qualified,³⁴ rel-

atively little is known about the extrapolation of *in vitro* data to the *in vivo* and an *in vivo* calibrator is not available for CYP2B6. It has been well-established in the literature that for CYP3A4, there is a strong correlation between mRNA and activity data.⁴⁸ This may not be the case for CYP2B6 due to the fact that CYP2B6 induction is CAR-mediated, whereas CYP3A4 induction is PXR-mediated. Here, *in vitro* CYP2B6 induction parameters based on CYP2B6 activity (hydroxybupropion formation) were used to drive the *in vivo* CYP2B6 induction without further calibration, and appeared to be successful in predicting both the autoinduction by efavirenz and the bupropion DDI. These data suggest that for IVIVE of CYP2B6 induction, an *in vivo* calibrator may not be necessary, although this awaits further confirmation by predicting the effect of other strong-to-moderate CYP2B6 inducers, including rifampin, carbamazepine, and ritonavir on bupropion PK from *in vitro* data.

In conclusion, the developed and verified model for efavirenz can be applied in clinical pharmacology studies to prospectively assess both the victim DDI potential (CYP2B6 induction) and perpetrator DDI potential (CYP2B6 and CYP3A4 induction) of efavirenz. Furthermore, we have demonstrated a recommended workflow for the development of PBPK models for complex drugs that induce their own metabolism as well as that of other (victim) drugs.

Acknowledgments. We thank Ming Zheng (Bristol Myers Squibb, Princeton, NJ) for providing efavirenz PK data for model development and verification, and Jane Kenny (Genentech, South San Francisco, CA) for the provision of efavirenz *in vitro* induction data. We also thank Eleanor Savill and Ruth Clayton for their assistance with manuscript preparation.

Conflict of Interest. All authors are paid employees of Simcyp Limited (a Certara company).

Author Contributions. A.K., Z.B., K.R.Y., and L.A. wrote the manuscript. A.K., K.R.Y., and L.A. designed the research. A.K., Z.B., and L.A. performed the research. A.K., Z.B., K.R.Y., and L.A. analyzed the data.

1. World Health Organisation. Consolidated guidelines on the use of antiretroviral drugs for treating and preventing HIV infection: recommendations for a public health approach. (2013). <<http://www.who.int/hiv/pub/guidelines/arv2013/download/en/>>.
2. Merck & Co. I. Crixivan (Indinavir Sulfate): prescribing information. (2002). <http://www.accessdata.fda.gov/drugsatfda_docs/label/2002/20685s050s053s056lbl.pdf>.
3. GlaxoSmithKline. Lexiva (Fosamprenavir Calcium): prescribing information. (2003). <http://www.accessdata.fda.gov/drugsatfda_docs/label/2003/21548_lexiva_lbl.pdf>.
4. GlaxoSmithKline. Tivicay (Dolutegravir): highlights of prescribing information. (2013). <http://www.accessdata.fda.gov/drugsatfda_docs/label/2013/204790lbl.pdf>.
5. Janssen. Olysio (Simeprevir): Highlights of prescribing information. (2013). <http://www.accessdata.fda.gov/drugsatfda_docs/label/2013/205123s000bletd.pdf>.
6. Merck & Co. I. Victrelis (Boceprevir): highlights of prescribing information. (2011). <http://www.accessdata.fda.gov/drugsatfda_docs/label/2011/202258lbl.pdf>.
7. US Food and Drug Administration, CDER. Olaparib clinical pharmacology review. (2014). <http://www.accessdata.fda.gov/drugsatfda_docs/nda/2014/206162Orig1s000ClinPharmR.pdf>.
8. US Food and Drug Administration, CDER. Naloxegol clinical pharmacology review. (2014). <http://www.accessdata.fda.gov/drugsatfda_docs/nda/2014/204760Orig1s000ClinPharmR.pdf>.
9. US Food and Drug Administration, CDER. Ibrutinib clinical pharmacology review. (2013). <http://www.accessdata.fda.gov/drugsatfda_docs/nda/2013/205552Orig1s000ClinPharmR.pdf>.
10. Schipani, A., Back, D., Owen, A., Davies, G., Khoo, S. & Siccardi, M. Use of *in vitro* to *in vivo* extrapolation to predict the optimal strategy for patients switching from efavirenz to maraviroc or nevirapine. *Clin. Pharmacokinet.* 54, 107–116 (2015).

11. Siccardi, M. *et al.* Use of a physiologically-based pharmacokinetic model to simulate artemether dose adjustment for overcoming the drug-drug interaction with efavirenz. *In Silico Pharmacol.* **1**, 4 (2013).
12. Siccardi, M. *et al.* Pharmacokinetic and pharmacodynamic analysis of efavirenz dose reduction using an in vitro-in vivo extrapolation model. *Clin. Pharmacol. Ther.* **92**, 494–502 (2012).
13. Liu, P., Foster, G., LaBadie, R.R., Gutierrez, M.J. & Sharma, A. Pharmacokinetic interaction between voriconazole and efavirenz at steady state in healthy male subjects. *J. Clin. Pharmacol.* **48**, 73–84 (2008).
14. Cho, D.Y., Ogburn, E.T., Jones, D. & Desta, Z. Contribution of N-glucuronidation to efavirenz elimination in vivo in the basal and rifampin-induced metabolism of efavirenz. *Antimicrob. Agents Chemother.* **55**, 1504–1509 (2011).
15. Ogburn, E.T., Jones, D.R., Masters, A.R., Xu, C., Guo, Y. & Desta, Z. Efavirenz primary and secondary metabolism in vitro and in vivo: identification of novel metabolic pathways and cytochrome P450 2A6 as the principal catalyst of efavirenz 7-hydroxylation. *Drug Metab. Dispos.* **38**, 1218–1229 (2010).
16. Kwara, A., Lartey, M., Sagoe, K.W., Rzek, N.L. & Court, M.H. CYP2B6 (c.516G→T) and CYP2A6 (*9B and/or *17) polymorphisms are independent predictors of efavirenz plasma concentrations in HIV-infected patients. *Br. J. Clin. Pharmacol.* **67**, 427–436 (2009).
17. Dickinson, L. *et al.* Pharmacokinetic and pharmacodynamic comparison of once-daily efavirenz (400 mg vs. 600 mg) in treatment-naïve HIV-infected patients: results of the ENCORE1 study. *Clin. Pharmacol. Ther.* **98**, 406–416 (2015).
18. Kharasch, E.D. *et al.* Mechanism of efavirenz influence on methadone pharmacokinetics and pharmacodynamics. *Clin. Pharmacol. Ther.* **91**, 673–684 (2012).
19. Zhu, M., Kaul, S., Nandy, P., Grasela, D.M. & Pfister, M. Model-based approach to characterize efavirenz autoinduction and concurrent enzyme induction with carbamazepine. *Antimicrob. Agents Chemother.* **53**, 2346–2353 (2009).
20. Robertson, S.M., Maldarelli, F., Natarajan, V., Formentini, E., Alfaro, R.M. & Penzak, S.R. Efavirenz induces CYP2B6-mediated hydroxylation of bupropion in healthy subjects. *J. Acquir. Immune Defic. Syndr.* **49**, 513–519 (2008).
21. Shou, M. *et al.* Modeling, prediction, and in vitro in vivo correlation of CYP3A4 induction. *Drug Metab. Dispos.* **36**, 2355–2370 (2008).
22. Rekić, D., Roshammam, D., Mukonzo, J. & Ashton, M. In silico prediction of efavirenz and rifampicin drug-drug interaction considering weight and CYP2B6 phenotype. *Br. J. Clin. Pharmacol.* **71**, 536–543 (2011).
23. Mouly, S. *et al.* Hepatic but not intestinal CYP3A4 displays dose-dependent induction by efavirenz in humans. *Clin. Pharmacol. Ther.* **72**, 1–9 (2002).
24. Oswald, S. *et al.* Impact of efavirenz on intestinal metabolism and transport: insights from an interaction study with ezetimibe in healthy volunteers. *Clin. Pharmacol. Ther.* **91**, 506–513 (2012).
25. Zhao, P., Rowland, M. & Huang, S.M. Best practice in the use of physiologically based pharmacokinetic modeling and simulation to address clinical pharmacology regulatory questions. *Clin. Pharmacol. Ther.* **92**, 17–20 (2012).
26. Sager, J.E., Yu, J., Ragueneau-Majlessi, I. & Isoherranen, N. Physiologically based pharmacokinetic (PBPK) modeling and simulation approaches: a systematic review of published models, applications, and model verification. *Drug Metab. Dispos.* **43**, 1823–1837 (2015).
27. Wagner, C., Pan, Y., Hsu, V., Sinha, V. & Zhao, P. Predicting the effect of CYP3A inducers on the pharmacokinetics of substrate drugs using physiologically based pharmacokinetic (PBPK) modeling: an analysis of PBPK submissions to the US FDA. *Clin. Pharmacokinet.* **55**, 475–483 (2015).
28. Abduljalil, K., Cain, T., Humphries, H. & Rostami-Hodjegan, A. Deciding on success criteria for predictability of pharmacokinetic parameters from in vitro studies: an analysis based on in vivo observations. *Drug Metab. Dispos.* **42**, 1478–1484 (2014).
29. Guest, E.J., Aarons, L., Houston, J.B., Rostami-Hodjegan, A. & Galetin, A. Critique of the two-fold measure of prediction success for ratios: application for the assessment of drug-drug interactions. *Drug Metab. Dispos.* **39**, 170–173 (2011).
30. Snoeys, J., Beumont, M., Monshouwer, M. & Ouwerkerk-Mahadevan, S. Mechanistic understanding of the nonlinear pharmacokinetics and intersubject variability of simeprevir: a PBPK-guided drug development approach. *Clin. Pharmacol. Ther.* **99**, 224–234 (2016).
31. Poulin, P. & Haddad, S. Advancing prediction of tissue distribution and volume of distribution of highly lipophilic compounds from a simplified tissue-composition-based model as a mechanistic animal alternative method. *J. Pharm. Sci.* **101**, 2250–2261 (2012).
32. Hyland, R., Dickins, M., Collins, C., Jones, H. & Jones, B. Maraviroc: in vitro assessment of drug-drug interaction potential. *Br. J. Clin. Pharmacol.* **66**, 498–507 (2008).
33. Takano, R. *et al.* Oral absorption of poorly water-soluble drugs: computer simulation of fraction absorbed in humans from a miniscale dissolution test. *Pharm. Res.* **23**, 1144–1156 (2006).
34. Almond, L.M. *et al.* Prediction of drug-drug interactions arising from CYP3A induction using a physiologically based dynamic model. *Drug Metab. Dispos.* **44**, 821–832 (2016).
35. Tanaka, R., Hanabusa, H., Kinai, E., Hasegawa, N., Negishi, M. & Kato, S. Intracellular efavirenz levels in peripheral blood mononuclear cells from human immunodeficiency virus-infected individuals. *Antimicrob. Agents Chemother.* **52**, 782–785 (2008).
36. Almond, L.M., Hoggard, P.G., Edirisinghe, D., Khoo, S.H. & Back, D.J. Intracellular and plasma pharmacokinetics of efavirenz in HIV-infected individuals. *J. Antimicrob. Chemother.* **56**, 738–744 (2005).
37. Balani, S.K., Kauffman, L.R., deLuna, F.A. & Lin, J.H. Nonlinear pharmacokinetics of efavirenz (DMP-266), a potent HIV-1 reverse transcriptase inhibitor, in rats and monkeys. *Drug Metab. Dispos.* **27**, 41–45 (1999).
38. Rabel, S.R., Maurin, M.B., Rowe, S.M. & Hussain, M. Determination of the pKa and pH-solubility behavior of an ionizable cyclic carbamate, (S)-6-chloro-4-(cyclopropylethynyl)-1,4-dihydro-4-(trifluoromethyl)-2H-3,1-benzoxazin-2-one (DMP 266). *Pharm. Dev. Technol.* **1**, 91–95 (1996).
39. Almond, L. *et al.* The relationship between mRNA and activity following induction of CYP3A4 and CYP2B6 across a range of prototypical inducers. Poster presented at: 20th North American ISSX Meeting; October 18–22, 2015; Orlando, FL.
40. Rowland Yeo, K., Jamei, M., Yang, J., Tucker, G.T. & Rostami-Hodjegan, A. Physiologically based mechanistic modelling to predict complex drug-drug interactions involving simultaneous competitive and time-dependent enzyme inhibition by parent compound and its metabolite in both liver and gut – the effect of diltiazem on the time-course of exposure to triazolam. *Eur. J. Pharm. Sci.* **39**, 298–309 (2010).
41. Xu, C., Ogburn, E.T., Guo, Y. & Desta, Z. Effects of the CYP2B6*6 allele on catalytic properties and inhibition of CYP2B6 in vitro: implication for the mechanism of reduced efavirenz metabolism and other CYP2B6 substrates in vivo. *Drug Metab. Dispos.* **40**, 717–725 (2012).
42. Jiang, F. *et al.* Effects of clopidogrel and itraconazole on the disposition of efavirenz and its hydroxyl metabolites: exploration of a novel CYP2B6 phenotyping index. *Br. J. Clin. Pharmacol.* **75**, 244–253 (2013).
43. Abel, S., Jenkins, T.M., Whitlock, L.A., Ridgway, C.E. & Muirhead, G.J. Effects of CYP3A4 inducers with and without CYP3A4 inhibitors on the pharmacokinetics of maraviroc in healthy volunteers. *Br. J. Clin. Pharmacol.* **65** Suppl 1, 38–46 (2008).
44. FDA, CDER. Sustiva Clinical Pharmacology and Biopharmaceutics Review. (2006). <http://www.accessdata.fda.gov/drugsatfda_docs/nda/98/20972.cfm>.
45. Xu, C. & Desta, Z. In vitro analysis and quantitative prediction of efavirenz inhibition of eight cytochrome P450 (CYP) enzymes: major effects on CYPs 2B6, 2C8, 2C9 and 2C19. *Drug Metab. Pharmacokinet.* **28**, 362–371 (2013).
46. Jones, H.M. *et al.* Physiologically based pharmacokinetic modeling in drug discovery and development: a pharmaceutical industry perspective. *Clin. Pharmacol. Ther.* **97**, 247–262 (2015).
47. Nishiya, Y. *et al.* Comparison of mechanism-based inhibition of human cytochrome P450 2C19 by ticlopidine, clopidogrel, and prasugrel. *Xenobiotica* **39**, 836–843 (2009).
48. Einolf, H.J. *et al.* Evaluation of various static and dynamic modeling methods to predict clinical CYP3A induction using in vitro CYP3A4 mRNA induction data. *Clin. Pharmacol. Ther.* **95**, 179–188 (2014).

© 2016 The Authors CPT: Pharmacometrics & Systems Pharmacology published by Wiley Periodicals, Inc. on behalf of American Society for Clinical Pharmacology and Therapeutics. This is an open access article under the terms of the Creative Commons Attribution-NonCommercial License, which permits use, distribution and reproduction in any medium, provided the original work is properly cited and is not used for commercial purposes.

Supplementary information accompanies this paper on the CPT: Pharmacometrics & Systems Pharmacology website (<http://www.wileyonlinelibrary.com/psp4>)